Volume 6 | Number 3 | March 2015 | Pages 1593–2124

Chemical Science

www.rsc.org/chemicalscience

ISSN 2041-6539

ROYAL SOCIETY OF CHEMISTRY

EDGE ARTICLE

Bo Wang, Ying-Wei Yang *et al.*

Stimuli-responsive metal–organic frameworks gated by pillar[5]arene supramolecular switches

Chemical Science

EDGE ARTICLE

View Article Online
View Journal | View Issue

Cite this: *Chem. Sci.*, 2015, **6**, 1640

Stimuli-responsive metal–organic frameworks gated by pillar[5]arene supramolecular switches†

Li-Li Tan,[a] Haiwei Li,[b] Yu-Chen Qiu,[a] Dai-Xiong Chen,[a] Xin Wang,[a] Rui-Yi Pan,[a] Yan Wang,[a] Sean Xiao-An Zhang,[a] Bo Wang*[b] and Ying-Wei Yang*[a]

Received 4th December 2014
Accepted 24th December 2014

DOI: 10.1039/c4sc03749a

www.rsc.org/chemicalscience

Spurred on by recent advances in materials chemistry and drug delivery, a new stimuli-responsive theranostic hybrid platform, based on mechanized monodisperse nano metal–organic frameworks (NMOFs) gated by carboxylatopillar[5]arene (CP5) switches with bio-friendly pH-triggered cargo release capabilities, has been constructed for the first time. This nanoscale smart cargo delivery system showed pH- and/or competitive binding agent-triggered controlled cargo release with negligible premature release, large pore sizes for drug encapsulation, low cytotoxicity, good biodegradability and biocompatibility, and potential application in cell imaging, which offers a new tool in targeted drug delivery and the controlled release of therapeutic agents.

Introduction

The past decade has witnessed the revolutionary impact of nanotechnology on modern nanomedicine, since advanced nanoscale systems can both alleviate many of the pitfalls associated with free drug therapeutics and improve the efficacy of conventional drugs.[1–4] In particular, stimuli-responsive functional nanocarriers[5,6] for drug delivery and controlled release hold great promise in achieving revolutionary advances in virtually all aspects of medicine, including *in vitro* diagnostics,[7,8] bioimaging,[9] targeted and internally/externally triggered therapy,[10–16] image-guided surgery, and regenerative medicine. Among advanced nanomaterials, metal–organic frameworks (MOFs)[17] have emerged as powerful platforms for gas storage,[18–20] catalysis,[21] separation,[22] drug delivery,[23–25] imaging,[26] sensors[27] and detection[28,29] owing to their tunable structural features and pore sizes, high surface areas, chemical/thermal stability, and versatile functionality. In particular, the biomedical application of MOFs[30] is gaining tremendous attention, especially in the field of nanomedicine, and this emerging class of porous materials is likely to replace traditional nanoporous materials in drug delivery and storage in the future, due to their unique properties such as exceptionally high surface areas and large pore sizes for drug encapsulation, good biodegradability and biocompatibility, versatile functionality, and potential application in cell imaging. However, to the best of our knowledge, no mechanized MOFs, which are composed of MOFs as scaffolds and supramolecular switches as gating entities to prevent premature cargo leakage and enable cargo release in a fine-tuned, targeted and controlled fashion, have so far demonstrated on-demand release of drugs.

In the human body, zinc plays "ubiquitous biological roles", such as maintaining the immune function, sterilization, and treatment of cancer, and is essential for the structural stability of a variety of proteins involved in transcription, protein trafficking, neurosecretory products or cofactors, and enzyme catalytic activity.[31] UMCM-1-NH_2 (UMCM = University of Michigan Crystalline Material) is a MOF 'co-polymer' constructed by combining zinc with both a two-fold symmetric (2-amino-1,4-benzenedicarboxylate, BDC-NH_2) and a three-fold symmetric (1,3,5-benzene-tri-*p*-benzoate, BTB) organic linker, which produces a hexagonal mesopore with a 1D hexagonal channel of 27 × 32 Å surrounded by six smaller polygonal micropores each with a dimension of 14 × 17 Å.[32] As the BDC-NH_2 linkers are located at the junctions of the microporous cages, the introduction of small functional groups as stalks to the linkers through post-synthetic modification (PSM) would mainly affect the pore environment of the cages, without affecting the porosity of the large channel.[33,34] Their large pore size and previous successes with PSM reactions make them promising candidates as nanocarriers for controlled drug delivery.

Pillar[*n*]arenes (pillarenes for short) as a relatively new class of synthetic macrocycles have seen a tremendous boost[35–39] in their use for host–guest chemistry in the last six years since they integrate the advantages of other existing macrocyclic host

[a]*State Key Laboratory of Supramolecular Structure and Materials, College of Chemistry, International Joint Research Laboratory of Nano-Micro Architecture Chemistry (NMAC), Jilin University, 2699 Qianjin Street, Changchun 130012, P. R. China. E-mail: ywyang@jlu.edu.cn; yyang@chem.ucla.edu*

[b]*Key Laboratory of Cluster Science, Ministry of Education of China School of Chemistry, Beijing Institute of Technology, 5 South Zhongguancun Street, Beijing, 100081, P. R. China. E-mail: bowang@bit.edu.cn*

† Electronic supplementary information (ESI) available: Experimental details, FTIR spectra, SEM and TEM images, characterization and controlled release experiments. See DOI: 10.1039/c4sc03749a

compounds and possess their own unique characteristics, which facilitate their applications in artificial transmembrane channels,[40,41] controlled release systems,[42–46] gas sorption,[47,48] MOFs,[49] sensing and detection,[50,51] stabilization of nanoparticles, and other typical biological applications,[52,53] *etc.*[54–60]

Herein, monodisperse mechanized nanoMOFs (NMOFs) with pillarene-based supramolecular switches as gatekeepers have been constructed by combining PSM of MOFs with stimuli-responsive host–guest chemistry on MOF surfaces for the first time (Fig. 1). This system has shown pH- and/or competitive binding-triggered controlled cargo release with negligible premature release, large pore sizes for drug encapsulation, very low cytotoxicity, good biodegradability and biocompatibility, and potential application in cell imaging, which will open a new avenue in targeted drug delivery and controlled release of therapeutic agents, especially in the treatment of degenerative diseases.

Results and discussion

The fabrication of the carboxylatopillar[5]arene (CP5)-based mechanized UMCM-1-NH_2 nanocarrier systems is depicted in Fig. 1. The scaffold UMCM-1-NH_2 was synthesized according to the literature procedure (ESI†).[32] Positively-charged pyridinium (Py) stalks were successfully tethered onto the UMCM-1-NH_2 surfaces *via* PSM, followed by the loading of luminescent rhodamine 6G (Rh6G, 1 mM) as a model drug in their nanopores at room temperature. Finally, the negatively-charged CP5 macrocycles were introduced to encircle the Py stalks *via* host–guest complexation to form [2]pseudorotaxanes as the movable elements of the mechanized nanocarriers, thereby realizing the drug encapsulation.

The peaks of Py in the ^{1}H NMR spectra (Fig. S7†) and the peak of BDC-NH–Py in the electrospray ionization mass spectrometry (ESI-MS, Fig. S8†) indicated that the Py stalks were successfully anchored to UMCM-1-NH_2. The conversion of the modification of UMCM-1-NH_2 was calculated to be 50%. Fourier transform infrared (FTIR) spectra (Fig. S9†) were also used to verify and monitor the functionalization of UMCM-1-NH_2. Compared to UMCM-1-NH_2, the presence of the peaks of –CH_2– (~2859 and ~2928 cm^{-1}), –NH– (~1283 cm^{-1}) and –C=N– (~1708 cm^{-1}) was indicative of the fact that UMCM-1-NH–Py was formed. Shift and intensity changes in peaks of the Rh6G-loaded, CP5-capped UMCM-1-NH–Py curve appeared at around 2900 cm^{-1} and peaks from 1700 cm^{-1} to 1000 cm^{-1} were caused by the encasing of CP5 and the loading of Rh6G. Meanwhile, thermogravimetric analysis (TGA) of UMCM-1-NH–Py showed a rapid weight loss (4%) first (Fig. S10†) which corresponds to the liberation of DMF molecules entrapped inside the cavity, followed by a plateau region until 325 °C, where the materials began decomposing, ascribed to the loss of Py. This certified UMCM-1-NH–Py to have enough thermal stability for constructing drug delivery systems. To further test the microcrystallinity of our newly synthesized functional materials, high-resolution transmission electron microscopy (HRTEM) images and electron-diffraction patterns were taken (Fig. 2 and S14†). HRTEM images indicated that both UMCM-1-NH_2 (Fig. 2b) and Rh6G-loaded, CP5-capped UMCM-1-NH–Py (Fig. 2e) have well-defined crystalline planes with interplanar *d*-spacing of 0.304 nm, corresponding to the lattice spacing of the (103) planes. Electron-diffraction patterns are a vivid demonstration of the single crystalline nature of these nanoparticles. Furthermore, the pore size distribution (Fig. S11 and S12†) was obtained using the non-localized DFT (NLDFT) method from N_2 sorption isotherms at 77 K. UMCM-1-NH–Py showed two main sharp peaks at approximately 1.7 nm and 4.6 nm consistent with UMCM-1-NH_2 and the crystal structure according to the literature[32] (Fig. S15†) which means that the pores of the nanoparticles were not changed after grafting pyridine units onto the openings of the pores by covalent bonds and the nanoparticles can be used as a drug carrier and further incorporated with supramolecular switches to construct nanovalves.

The morphology, size, monodispersity, and surface texture of these nanoparticles were investigated by scanning electron

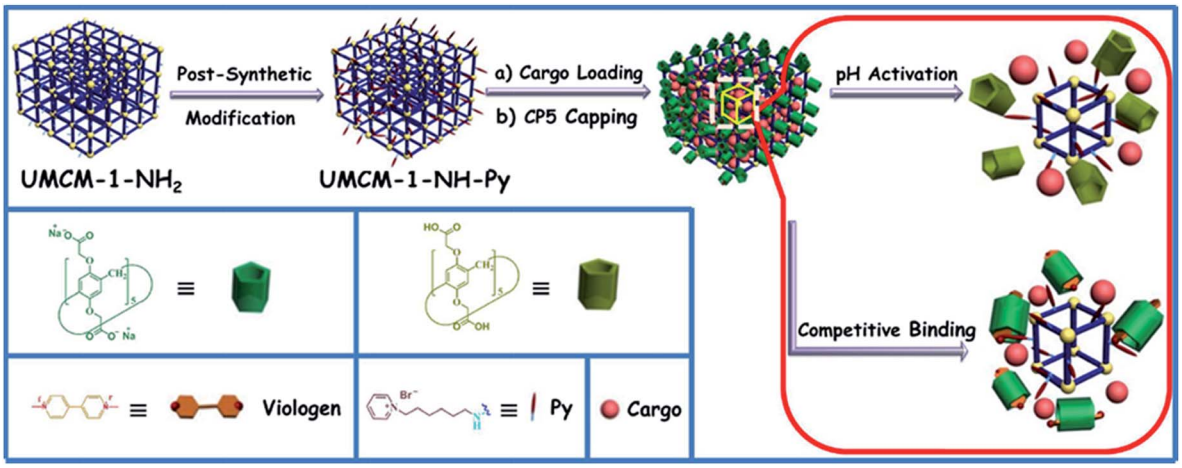

Fig. 1 Schematic representation of stimuli-responsive nanocarriers based on mechanized nanoMOFs (UMCM-1-NH_2) with positively-charged pyridinium units (Py) as stalks encircled by pillarenes on the surfaces. The mechanized UMCM-1-NH_2 nanovalves can be operated either by pH changes or by competitive binding to regulate the release of cargo molecules, *i.e.*, rhodamine 6G (Rh6G) and doxorubicin hydrochloride (DOX).

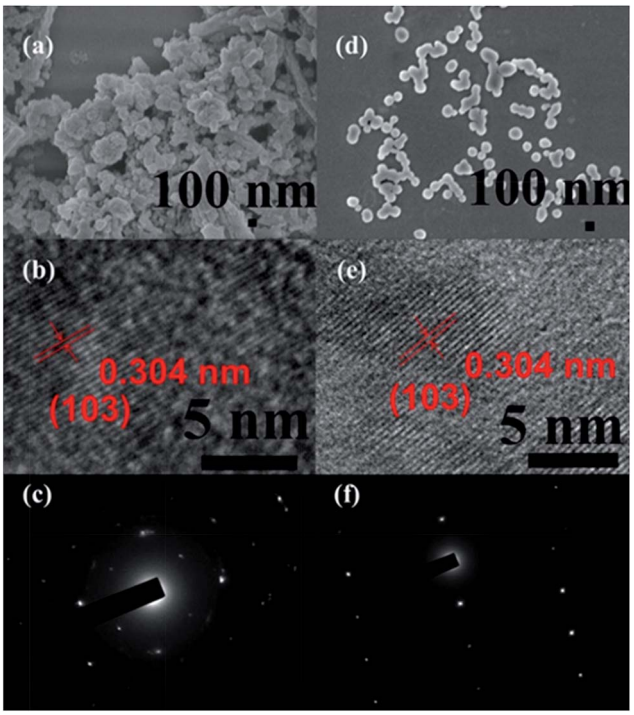

Fig. 2 (a) SEM image of UMCM-1-NH_2, (b) HRTEM image of UMCM-1-NH_2, (c) the corresponding electron diffraction pattern of UMCM-1-NH_2, (d) SEM image of Rh6G-loaded, CP5-capped UMCM-1-NH–Py, (e) HRTEM image of Rh6G-loaded, CP5-capped UMCM-1-NH–Py, and (f) the corresponding electron diffraction pattern of Rh6G-loaded, CP5-capped UMCM-1-NH–Py.

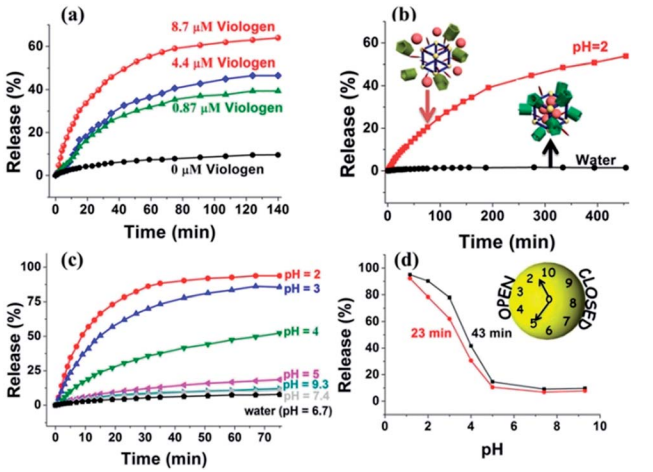

Fig. 3 Release profiles of the Rh6G-loaded, CP5-capped UMCM-1-NH–Py operated by (a) competitive binding, *i.e.*, addition of viologen and (c) pH changes. (b) Release profiles of the DOX-loaded, CP5-capped UMCM-1-NH–Py operated by pH activation. (d) The amount of Rh6G released as a function of pH at 23 and 43 min from the Rh6G-loaded, CP5-capped UMCM-1-NH–Py by changing the pH; inset is a pH clock.

microscope (SEM), dynamic light scattering (DLS), and zeta potential measurements. Zeta potentials are displayed in Table S1,† showing that UMCM-1-NH–Py has positive surface charges and Rh6G-loaded, CP5-capped UMCM-1-NH–Py has negative surface charges, which further validated the successful modification and capping. The zeta potential of Rh6G-loaded, CP5-capped UMCM-1-NH–Py was measured to be −16.4 mV which clearly revealed that the newly synthesized drug delivery system can maintain certain stability and is strong enough to transport drugs successfully in biological media. DLS was used to calculate the average diameter of the NMOFs in water. In particular, the average particle size (Table S1†) in solution became progressively smaller after modification and capping due to the good solubility of Py and CP5 in water. The average particle diameter of Rh6G-loaded, CP5-capped UMCM-1-NH–Py was calculated to be 102.9 nm, which is within the size range[61] for easy uptake by cells. Interestingly, the nanoparticles became monodisperse with homogeneous particle sizes (*ca.* 102 nm), evidenced by SEM (Fig. 2d), which makes the mechanical nanocarriers constructed from UMCM-1-NH–Py and CP5 promising candidates for drug storage and drug delivery.

Upon addition of methyl viologen salts, which have a higher binding affinity toward CP5 ($K_a \approx 8 \times 10^4\ M^{-1}$),[62] into a cuvette containing Rh6G-loaded, CP5-capped UMCM-1-NH–Py, an immediate release of the cargo molecules was observed (Fig. 3a) as a result of the methyl viologen-induced dethreading of the CP5 rings from the Py stalk components ($K_a = (2.5 \pm 0.7) \times 10^3\ M^{-1}$).[61] The release rate of Rh6G depends on the amount of methyl viologen salts added, which indicated the important role of the CP5 supramolecular switches.

Neutralization of the CP5 sodium salts upon lowering the pH of the solution results in the weakening of the noncovalent bonding interactions between the ring and stalk components of the CP5[2]pseudorotaxanes, leading to the unblocking of the nanopores.[61] So, Rh6G-loaded, CP5-capped UMCM-1-NH–Py nanoparticles were able to contain Rh6G molecules at neutral pH and basic pH (Fig. 3c), but release them under acidic pH and the release rate of Rh6G depends on the pH level like a pH clock[63] (Fig. 3d). A flat baseline shows (Fig. 3c) that the molecules of Rh6G are held firmly within the nanopores at neutral pH and basic pH: there is no premature release, which is a breakthrough for MOF-based drug delivery systems. When the pH of the solution is lowered to 5, the supramolecular nanovalves are opened and the cargo of Rh6G molecules is released. The lower the pH (*e.g.*, 2), the faster the release of the cargo. Meanwhile, the anticancer drug, doxorubicin hydrochloride (DOX), was loaded into the nanopores: a smooth release profile was observed (Fig. 3b) upon lowering the pH. As pH in areas of tumor tissues is known to be more acidic than in blood and normal tissues (pH 7.4) and in view of the fact that their lysosomal pH levels are somewhat lower than in healthy human cells, a pH responsive drug delivery system can reduce undesired drug release during drug transportation in blood circulation and improve the effective release of the antitumor drug in the tumor tissue or within tumor cells.[63] What's more, since the drug is expected to be released much faster at the tumor site than the surrounding normal tissues maintaining a physiological pH of 7.4, it is expected that the delivery of chemotherapeutic drugs *via* these systems may also reduce their adverse effects which in some cases can be severely debilitating. So, with

no doubt, pH-sensitive carriers are particularly promising candidates for anticancer drug delivery.

A series of control experiments have also been done to prove the functionalization of CP5 supramolecular switches in the UMCM-1-NH–Py drug delivery system by comparing the difference of the release performance of Rh6G-loaded, CP5-capped UMCM-1-NH–Py and Rh6G-loaded UMCM-1-NH_2 without CP5 capping by pH activation (Fig. S5†). Premature leakage without the CP5 rings attached was more obvious than that with the CP5 rings and the encapsulation efficiency of the MOFs without the CP5 rings attached (5 μmol g^{-1}) was significantly lower than that with the CP5 rings (61 μmol g^{-1}). These reveal the important role of CP5 supramolecular switches in our system for tuning the drug loading capacity.

As shown in Fig. S16,† with the increase in concentration of the two nanomaterials, the cell viabilities showed a declining trend. However, they only had slight cytotoxicity to normal human cells, which was deduced from the fact that the cell viabilities were higher than 60%, even though their concentration was as high as 50 μg mL^{-1}. Overall, the nanomaterials, before and after capping with CP5, possess negligible cell cytotoxicity at low concentrations, allowing them to be used as nanocontainers for controlled drug delivery in disease therapy.

Conclusions

In conclusion, monodisperse mechanized nanocarriers based on NMOFs and pillarene-based supramolecular switches as gatekeepers have been constructed for the first time by combining PSM with stimuli-responsive host–guest chemistry. UMCM-1-NH_2 with mesopores (27 × 32 Å) and micropores (14 × 17 Å) was selected as a nanocontainer and positively-charged Py stalks were successfully attached to the UMCM-1-NH_2 *via* PSM without affecting the porosity of the large channel, which was confirmed by ^{1}H NMR, ESI-MS, FTIR spectra and pore size distribution. Then, Rh6G and DOX were loaded, negatively charged CP5 macrocycles were introduced to encircle the Py stalks *via* host–guest complexation to form [2]pseudorotaxanes as the movable elements of the nanocarriers, thereby realizing the drug encapsulation. HRTEM, SEM, zeta potential, and DLS showed that this mechanical nanocontainer is mainly in monodisperse microcrystalline form, certainly stable and within the size range that can be easily taken up by cells (102 nm). MTT cytotoxicity assay of 293 cells treated with UMCM-1-NH–Py and CP5-capped UMCM-1-NH–Py at various concentrations conveyed that the new functional materials, before and after CP5 capping, possess negligible cytotoxicity. This unique MOF-based nanovalve system showed pH- and/or competitive binding agent-triggered controlled cargo release with negligible premature release, large pore sizes for drug encapsulation, non-cytotoxicity, good biodegradability and biocompatibility, and potential application in cell imaging, which will open new avenues in targeted drug delivery and controlled release of therapeutic agents, especially in the treatment of cancer diseases. Future investigations will employ this integrated nanosystem to carry anticancer drugs, perform pH-responsive drug release *in vivo*, take advantage of the properties of the metal and organic ligands it contains, and could one day find application in excellent treatment of human cancers.

Acknowledgements

This research is supported by the National Natural Science Foundation of China (21272093 and 51473061), the Specialized Research Fund for the Doctoral Program of Higher Education of China (20120061120117), the Fundamental Research Funds for the Central Universities (no. JCKY-QKJC05), the Innovation Program of the State Key Laboratory of Supramolecular Structure and Materials, and the National Science Foundation for Fostering Talents in Basic Research of the National Natural Science Foundation of China (grant no. J1103302).

Notes and references

1 Y.-W. Yang, Y.-L. Sun and N. Song, *Acc. Chem. Res.*, 2014, **47**, 1950.
2 J. A. Hubbell and A. Chilkoti, *Science*, 2012, **337**, 303.
3 V. Valtchev and L. Tosheva, *Chem. Rev.*, 2013, **113**, 6734.
4 M. Zhang, Z.-Y. Gu, M. Bosch, Z. Perry and H.-C. Zhou, *Coord. Chem. Rev.*, 2014, DOI: 10.1016/j.ccr.2014.05.031.
5 S. Angelos, Y.-W. Yang, N. M. Khashab, J. F. Stoddart and J. I. Zink, *J. Am. Chem. Soc.*, 2009, **131**, 11344.
6 T. D. Nguyen, Y. Liu, S. Saha, K. C.-F. Leung, J. F. Stoddart and J. I. Zink, *J. Am. Chem. Soc.*, 2007, **129**, 626.
7 Q.-L. Li, Y. Sun, Y.-L. Sun, J. Wen, Y. Zhou, Q.-M. Bing, L. D. Isaacs, Y. Jin, H. Gao and Y.-W. Yang, *Chem. Mater.*, 2014, **26**, 6418.
8 C. R. Thomas, D. P. Ferris, J.-H. Lee, E. Choi, M. H. Cho, E. S. Kim, J. F. Stoddart, J.-S. Shin, J. Cheon and J. I. Zink, *J. Am. Chem. Soc.*, 2010, **132**, 10623.
9 M. Liong, S. Angelos, E. Choi, K. Patel, J. F. Stoddart and J. I. Zink, *J. Mater. Chem.*, 2009, **19**, 6251.
10 Y.-L. Sun, Y. Zhou, Q.-L. Li and Y.-W. Yang, *Chem. Commun.*, 2013, **49**, 9033.
11 H. Li, L.-L. Tan, P. Jia, Q.-L. Li, Y.-L. Sun, J. Zhang, Y.-Q. Ning, J. Yu and Y.-W. Yang, *Chem. Sci.*, 2014, **5**, 2804.
12 Y. Zhou, L.-L. Tan, Q.-L. Li, X.-L. Qiu, A.-D. Qi, Y. Tao and Y.-W. Yang, *Chem.–Eur. J.*, 2014, **20**, 2998.
13 A. C. Fahrenbach, S. C. Warren, J. T. Incorvati, A.-J. Avestro, J. C. Barnes, J. F. Stoddart and B. A. Grzybowski, *Adv. Mater.*, 2013, **3**, 331.
14 Q. He and J. Shi, *Adv. Mater.*, 2014, **26**, 391.
15 Y.-R. Zheng, K. Suntharalingam, T. C. Johnstone and S. J. Lippard, *Chem. Sci.*, 2015, DOI: 10.1039/c4sc01892c.
16 K. Patel, S. Angelos, W. R. Dichtel, A. Coskun, Y.-W. Yang, J. I. Zink and J. F. Stoddart, *J. Am. Chem. Soc.*, 2008, **130**, 2382.
17 S. T. Meek, J. A. Greathouse and M. D. Allendorf, *Adv. Mater.*, 2011, **23**, 249.
18 K. Sumida, D. L. Rogow, J. A. Mason, T. M. McDonald, E. D. Bloch, Z. R. Herm, T.-H. Bae and J. R. Long, *Chem. Rev.*, 2012, **112**, 724.
19 J. Park, L.-B. Sun, Y.-P. Chen, Z. Perry and H.-C. Zhou, *Angew. Chem., Int. Ed.*, 2014, **53**, 5842.

20 J. Y. Lee, L. Pan, S. P. Kelly, J. Jagiello, T. J. Emge and J. Li, *Adv. Mater.*, 2005, **17**, 2703.
21 J. Lee, O. K. Farha, J. Roberts, K. A. Scheidt, S. T. Nguyen and J. T. Hupp, *Chem. Soc. Rev.*, 2009, **38**, 1450.
22 J.-R. Li, J. Sculley and H.-C. Zhou, *Chem. Rev.*, 2012, **112**, 869.
23 P. Horcajada, C. Serre, M. Vallet-Regí, M. Sebban, F. Taulelle and G. Férey, *Angew. Chem., Int. Ed.*, 2006, **45**, 5974.
24 J. An, S. J. Geib and N. L. Rosi, *J. Am. Chem. Soc.*, 2009, **131**, 8376.
25 R. Ananthoji, J. F. Eubank, F. Nouar, H. Mouttaki, M. Eddaoudi and J. P. Harmon, *J. Mater. Chem.*, 2011, **21**, 9587.
26 K. M. L. Taylor-Pashow, J. D. Rocca, Z. Xie, S. Tran and W. Lin, *J. Am. Chem. Soc.*, 2009, **131**, 14261.
27 L. E. Kreno, K. Leong, O. K. Farha, M. Allendorf, R. P. Van Duyne and J. T. Hupp, *Chem. Rev.*, 2012, **112**, 1105.
28 Y. Guo, X. Feng, T. Han, S. Wang, Z. Lin, Y. Dong and B. Wang, *J. Am. Chem. Soc.*, 2014, **136**, 15485.
29 H. Li, X. Feng, Y. Guo, D. Chen, R. Li, X. Ren, X. Jiang, Y. Dong and B. Wang, *Sci. Rep.*, 2014, **4**, 4366.
30 P. Horcajada, R. Gref, T. Baati, P. K. Allan, G. Maurin, P. Couvreur, G. Férey, R. E. Morris and C. Serre, *Chem. Rev.*, 2012, **112**, 1232.
31 Á. Zotter, J. Oláh, E. Hlavanda, A. Bodor, A. Perczel, K. Szigeti, J. Fidy and J. Ovádi, *Biochemistry*, 2011, **50**, 9568.
32 Z. Wang, K. K. Tanabe and S. M. Cohen, *Inorg. Chem.*, 2009, **48**, 296.
33 G. Tuci, A. Rossin, X. Xu, M. Ranocchiari, J. A. Bokhoven, L. Luconi, I. Manet, M. Melucci and G. Giambastiani, *Chem. Mater.*, 2013, **25**, 2297.
34 Z. Wang and S. M. Cohen, *J. Am. Chem. Soc.*, 2009, **131**, 16675.
35 M. Xue, Y. Yang, X. Chi, Z. Zhang and F. Huang, *Acc. Chem. Res.*, 2012, **45**, 1294.
36 C. Li, *Chem. Commun.*, 2014, **50**, 12420.
37 T. Ogoshi and T. Yamagishi, *Chem. Commun.*, 2014, **50**, 4776.
38 N. Song and Y.-W. Yang, *Sci. China: Chem.*, 2014, **57**, 1185.
39 L.-L. Tan and Y.-W. Yang, *J. Inclusion Phenom. Macrocyclic Chem.*, 2015, DOI: 10.1007/s10847-014-0441-3.
40 W. Si, Z.-T. Li and J.-L. Hou, *Angew. Chem., Int. Ed.*, 2014, **53**, 4578.
41 L. Chen, W. Si, L. Zhang, G. Tang, Z.-T. Li and J.-L. Hou, *J. Am. Chem. Soc.*, 2013, **135**, 2152.
42 H. Zhang, X. Ma, K. T. Nguyen and Y. Zhao, *ACS Nano*, 2013, **7**, 7853.
43 Y. Yao, M. Xue, J. Chen, M. Zhang and F. Huang, *J. Am. Chem. Soc.*, 2012, **134**, 15712.
44 Q. Duan, Y. Cao, Y. Li, X. Hu, T. Xiao, C. Lin, Y. Pan and L. Wang, *J. Am. Chem. Soc.*, 2013, **135**, 10542.
45 Y. Cao, X.-Y. Hu, Y. Li, X. Zou, S. Xiong, C. Lin, Y.-Z. Shen and L. Wang, *J. Am. Chem. Soc.*, 2014, **136**, 10762.
46 G. Yu, X. Zhou, Z. Zhang, C. Han, Z. Mao, C. Gao and F. Huang, *J. Am. Chem. Soc.*, 2012, **134**, 19489.
47 L.-L. Tan, H. Li, Y. Tao, S. X.-A. Zhang, B. Wang and Y.-W. Yang, *Adv. Mater.*, 2014, **26**, 7027.
48 T. Ogoshi, R. Sueto, K. Yoshikoshi and T. Yamagishi, *Chem. Commun.*, 2014, **50**, 15209.
49 N. L. Strutt, D. Fairen-Jimenez, J. Iehl, M. B. Lalonde, R. Q. Snurr, O. K. Farha, J. T. Hupp and J. F. Stoddart, *J. Am. Chem. Soc.*, 2012, **134**, 17436.
50 H. Li, D.-X. Chen, Y.-L. Sun, Y. B. Zheng, L.-L. Tan, P. S. Weiss and Y.-W. Yang, *J. Am. Chem. Soc.*, 2013, **135**, 1570.
51 Y. Yao, X. Chi, Y. Zhou and F. Huang, *Chem. Sci.*, 2014, **5**, 2778.
52 G. Yu, Y. Ma, C. Han, Y. Yao, G. Tang, Z. Mao, C. Gao and F. Huang, *J. Am. Chem. Soc.*, 2013, **135**, 10310.
53 D.-D. Zheng, D.-Y. Fu, Y.-Q. Wu, Y.-L. Sun, L.-L. Tan, T. Zhou, S.-Q. Ma, X. Zha and Y.-W. Yang, *Chem. Commun.*, 2014, **50**, 3201.
54 Z.-Y. Li, Y. Zhang, C.-W. Zhang, L.-J. Chen, C. Wang, H. Tan, Y. Yu, X. Li and H.-B. Yang, *J. Am. Chem. Soc.*, 2014, **136**, 8577.
55 N. Song, D.-X. Chen, Y.-C. Qiu, X.-Y. Yang, B. Xu, W. Tian and Y.-W. Yang, *Chem. Commun.*, 2014, **50**, 8231.
56 K. Wang, C.-Y. Wang, Y. Zhang, S. X.-A. Zhang, B. Yang and Y.-W. Yang, *Chem. Commun.*, 2014, **50**, 9458.
57 X. Hou, C. Ke, C. Cheng, N. Song, A. K. Blackburn, A. A. Sarjeant, Y. Y. Botros, Y.-W. Yang and J. F. Stoddart, *Chem. Commun.*, 2014, **50**, 6196.
58 N. Song, D.-X. Chen, M.-C. Xia, X.-L. Qiu, K. Ma, B. Xu, W. Tian and Y.-W. Yang, *Chem. Commun.*, 2015, DOI: 10.1039/c4cc08205b.
59 J.-F. Xu, Y.-Z. Chen, L.-Z. Wu, C.-H. Tung and Q.-Z. Yang, *Org. Lett.*, 2013, **15**, 6148.
60 Y. Wang, J.-F. Xu, Y.-Z. Chen, L.-Y. Niu, L.-Z. Wu, C.-H. Tung and Q.-Z. Yang, *Chem. Commun.*, 2014, **50**, 7001.
61 Y.-L. Sun, Y.-W. Yang, D.-X. Chen, G. Wang, Y. Zhou, C.-Y. Wang and J. F. Stoddart, *Small*, 2013, **9**, 3224.
62 T. Ogoshi, M. Hashizume, T. Yamagishi and Y. Nakamoto, *Chem. Commun.*, 2010, **46**, 3708.
63 S. Angelos, N. M. Khashab, Y.-W. Yang, A. Trabolsi, H. A. Khatib, J. F. Stoddart and J. I. Zink, *J. Am. Chem. Soc.*, 2009, **131**, 12912.